AJNR

Prenatal Evaluation of Intracranial Hemorrhage on Fetal MRI: A Retrospective Review

K.N. Epstein, B.M. Kline-Fath, B. Zhang, C. Venkatesan, M. Habli, D. Dowd and U.D. Nagaraj

Prenatal Evaluation of Intracranial Hemorrhage on Fetal MRI: A Retrospective Review

K.N. Epstein, B.M. Kline-Fath, B. Zhang, C. Venkatesan, M. Habli, D. Dowd, and U.D. Nagaraj

ABSTRACT

BACKGROUND AND PURPOSE: The evaluation and characterization of germinal matrix hemorrhages have been predominantly described on postnatal head sonography in premature neonates. However, germinal matrix hemorrhages that are seen in premature neonates can be also seen in fetuses of the same postconceptual age and are now more frequently encountered in the era of fetal MR imaging. Our aim was to examine and describe the MR imaging findings of fetuses with intracranial hemorrhage.

MATERIALS AND METHODS: A retrospective review of diagnostic-quality fetal MRIs showing intracranial hemorrhage from January 2004 to May 2020 was performed. Images were reviewed by 2 radiologists, and imaging characteristics of fetal intracranial hemorrhages were documented. Corresponding postnatal imaging and clinical parameters were reviewed.

RESULTS: One hundred seventy-seven fetuses with a mean gestational age of 25.73 (SD, 5.01) weeks were included. Germinal matrix hemorrhage was identified in 60.5% (107/177) and nongerminal matrix hemorrhage in 39.5% (70/177) of patients. Significantly increased ventricular size correlated with higher germinal matrix hemorrhage grade ($P < .001$). Fetal growth restriction was present in 21.3% (20/94) of our population, and there was no significant correlation with germinal matrix grade or type of intracranial hemorrhage. An increased incidence of neonatal death with grade III germinal matrix hemorrhages ($P = .069$) compared with other grades was identified; 23.2% (16/69) of the neonates required ventriculoperitoneal shunts, with an increased incidence in the nongerminal matrix hemorrhage group ($P = .026$).

CONCLUSIONS: MR imaging has become a key tool in the diagnosis and characterization of intracranial hemorrhage in the fetus. Appropriate characterization is important for optimizing work-up, therapeutic approach, and prenatal counseling.

ABBREVIATIONS: GA = gestational age; GMH = germinal matrix hemorrhage; ICH = intracranial hemorrhage; SSFSE = single-shot fast spin-echo; US = sonography

Fetal MR imaging has become a valuable tool in the prenatal evaluation of the brain and has an important role in prenatal diagnosis and guiding prenatal/perinatal management and counseling.[1-3] MR imaging of the fetus has enabled the evaluation of parenchymal abnormalities that are not identified on sonography (US) and also confirms and elucidates the presence of intracranial hemorrhage (ICH).

Fetal ICH is rare, with an estimated incidence of 0.6–1/1000 cases.[4-6] The most common type of ICH in the fetus involves the germinal matrix, accounting for approximately two-thirds of cases, with the remainder involving non-germinal matrix hemorrhage locations.[7] Although the commonly used Burstein and Papile grading system was initially described on CT, the evaluation and characterization of germinal matrix hemorrhages (GMHs) have been predominantly described and classified on postnatal head US in premature neonates.[8,9] There is a 25%–40% reported incidence of GMH in premature neonates younger than 32 weeks' gestational age (GA) and those with a birth weight of <1500 grams.[10] However, GMHs that are seen in premature neonates can be also seen in fetuses of the same postconceptual age and are now more frequently encountered in the era of fetal MR imaging. GMH may result in considerable fetal and neonatal mortality and long-term neurologic morbidity in those neonates that survive, especially in the setting of grade III and IV GMHs.[11]

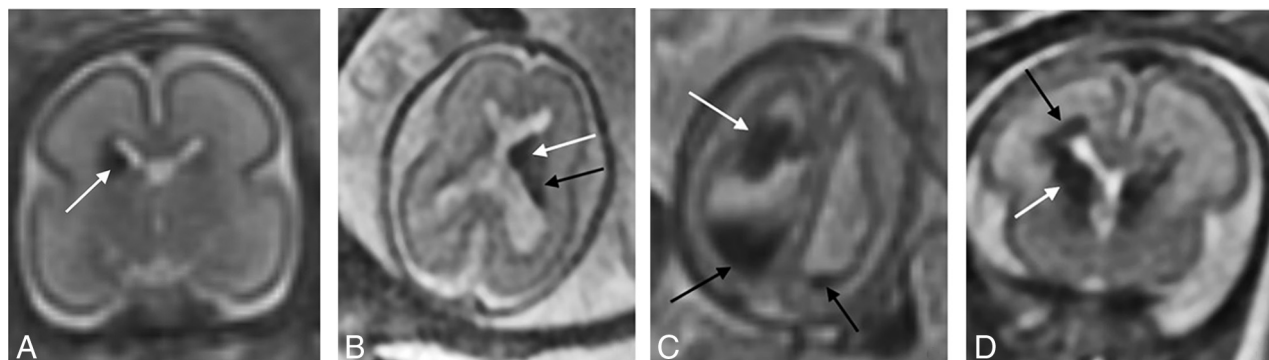Our aim was to examine the MR imaging findings of fetuses with intracranial hemorrhage.

FIG 1. *A*, Grade I GMH in a 24 -weeks' GA fetus. Coronal T2 SSFSE of the brain demonstrates T2 hypointensity at the right caudothalamic groove (*white arrow*). *B*, Grade II GMH in a 24 weeks' GA fetus. Axial T2 SSFSE of the brain shows T2 hypointensity at the left caudothalamic groove (*white arrow*) extending posteriorly along the margin of the lateral ventricle (*black arrow*). *C*, Grade III GMH in a 20 weeks' GA fetus. Axial T2 SSFSE of the brain demonstrates globular T2 hypointensity near the right caudothalamic groove (*white arrow*) with layering T2 hypointensity/hemorrhage in the right greater than left posterior horns of the ventricles (*black arrows*). There is dilation of the bilateral ventricles, right greater than left, measuring up to 16 mm on the right. *D*, Grade IV GMH in a 26 weeks' GA fetus. Coronal T2 SSFSE of the brain shows T2 hypointensity at the right caudothalamic groove (*white arrow*), with T2 signal/hemorrhage extending into the periventricular white matter (*black arrow*). Grade II GMH is partially visualized on the left.

MATERIALS AND METHODS

Study Design

This study is a single-center retrospective chart review. The case list was compiled using Illuminate InSight software (Softek Illuminate) from January 2004 through May 2020 ($n = 219/6179$). Inclusion criteria were fetuses with diagnostic-quality fetal MR images demonstrating intracranial hemorrhage ($n = 177$), with 42 fetuses excluded. All studies were reviewed by a pediatric radiology fellow and pediatric neuroradiologist to confirm the imaging findings in the radiology report. Determination of diagnostic-quality imaging was made at the discretion of the neuroradiologist and fellow radiologist. All images were viewed in the PACS workstation. A chart review was performed to obtain relevant clinical data. This study was compliant with the Health Insurance Portability and Accountability Act and was approved by the institutional review board. The requirement for informed consent was waived.

Scanning Parameters

All fetuses included in our study were scanned prenatally on a 1.5T magnet at Cincinnati Children's Hospital Medical Center using an Ingenia 1.5T scanner (Philips Healthcare) or a 1.5T Signa HDxt (GE Healthcare) system. The routinely implemented fetal brain protocol included axial, sagittal, and coronal T2-single-shot fast spin-echo (SSFSE) and balanced fast-field echo/FIESTA images. A section thickness of 3-mm, no-gap, interleaved images at ≤24 weeks' GA, and 4-mm, no-gap, interleaved images at >24 weeks' GA were used. Axial T1, DWI, and EPI blood sequences of the fetal brain were also variably obtained, routinely implemented in July 2016. The TR and TE varied on each scanner and were changed at times of scanner upgrades to optimize image quality. At least 2 stacks of images in each plane were obtained to the radiologists' satisfaction. The smallest FOV possible was used.

Image Interpretation

Fetal brain MR images and postnatal neuroimaging were reviewed by a board-eligible pediatric radiology fellow (K.N.E.) and a board-certified radiologist (U.D.N.) with added qualifications in pediatric radiology and neuroradiology and >5 years of postfellowship attending experience in a large academic center.

Fetuses that were determined to have ICH on diagnostic-quality fetal MR imaging were recorded. Fetal ICH imaging characteristics that were documented included presence vs absence of associated T2-SSFSE, T1, DWI, and EPI signal. Hemorrhages were classified as GMH versus non-GMH, depending on location. The non-GMH group included fetuses with a layering intraventricular blood product with a normal appearance of the fetal germinal matrix (ie, in setting of Chiari II malformation), parenchymal hemorrhages in the cerebellum or cerebrum without clear intraventricular extension, and extra-axial hemorrhages. GMHs were subsequently graded by the Burstein and Papile Modified Grading System as follows: grade I, subependymal hemorrhage; grade II, intraventricular hemorrhage filling <50% of the ventricle a with ventricular size of ≤15 mm; grade III, intraventricular hemorrhage filling >50% of the ventricle with a ventricular size of ≥15 mm; and grade IV, intraparenchymal periventricular hemorrhage in the setting of grades I–III GMH (Fig 1).[8] The location of the hemorrhage was documented. Fetuses with subependymal cysts, believed to be the result of prior GMH, were also documented as grade zero (Fig 2). Cerebellar hemorrhages were reported separate from the GMH classification if there was not additional hemorrhage localized to the caudothalamic groove (Fig 3). Additional imaging parameter that was recorded included lateral ventricular size, by measuring the transverse atrial diameter on an axial or coronal image.[12] The presence or absence of a 2-versus-3 vessel umbilical cord, placental abnormality, and other fetal structural abnormalities was recorded.

The reports of fetal sonographic studies performed at Cincinnati Children's Hospital Medical Center or outside institutions were reviewed when available. The presence or absence of fetal growth restriction (estimated fetal weight less than the 10th percentile), large for gestational age (estimated fetal weight greater than the 90th percentile for GA), abnormal findings on fetal Doppler, and twin-twin transfusion syndrome was recorded.[13,14] For the purposes of this study, abnormal findings on fetal Doppler included the following:
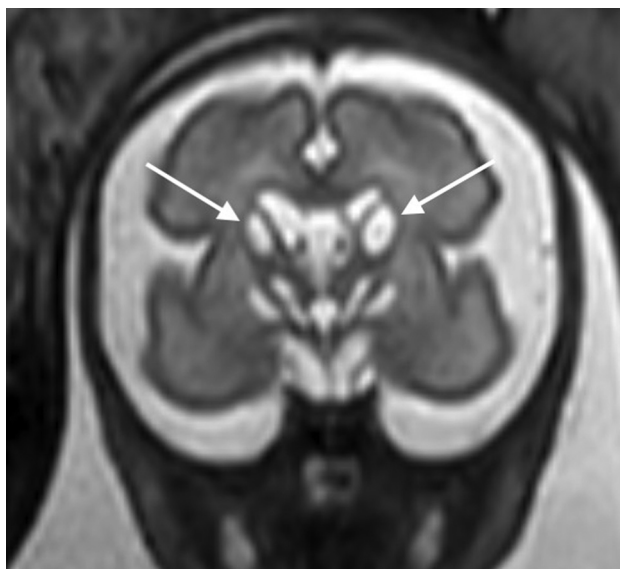
FIG 2. Grade 0 GMH in a 29 weeks' GA fetus. Coronal T2 SSFSE of the brain shows T2-hyperintense cystic lesions at the bilateral caudothalamic grooves (*white arrows*) and abnormal T2 hyperintense signal in the bilateral basal ganglia.
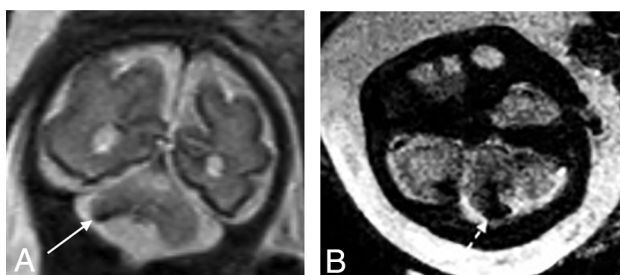

FIG 3. Coronal T2 SSFSE (*A*) and axial EPI (*B*) of the brain in a 31 weeks' GA fetus. Note T2 hypointensity at the margin of the inferior aspect of the deficient right cerebellar hemisphere (*arrow, A*) and an associated magnetic susceptibility signal at the right cerebellar hemisphere (*dashed arrow, B*) and vermis.

absent or reversal of diastolic flow in the umbilical artery; pulsatile umbilical vein; decreased, absent, or reversal of the a-wave in the ductus venosus; and/or elevated peak systolic velocity in the middle cerebral artery of >1.5 multiple of the mean.[14,15] Available postnatal neuroimaging was reviewed, including neonatal head US, brain MR imaging, and head CT. Imaging findings of ICH, neonatal brain parenchyma, and ventricular size were compared with the fetal MR imaging to assess whether there was interval worsening, stability, or improvement. Clinical parameters included the following: age of the mother, GA of the fetus at fetal MR imaging, sex of the fetus, singleton-versus-twin pregnancy, delivery outcome (death versus live birth), neonatal outcome (died versus alive after a live birth in the neonatal period), age at postnatal imaging, and the need for CSF diversion (shunting).

Statistical Analysis
Descriptive analyses were performed to demonstrate the distribution of the imaging findings. Continuous variables were presented

Table 1: Summary of cohort

Characteristics	Data (n = 177)
Sex	
Male	48.0% (85/177)
Female	40.1% (71/177)
Unknown	11.9% (21/177)
Singleton	70.1% (124/177)
Multiple gestation	29.9% (53/177)
Average GA at fetal MR imaging (wk)	25.73 (SD, 5.01)
GMH	60.5% (107/177)
Grade 0	12.1% (13/107)
Grade I	28.9% (31/107)
Grade II	28.0% (30/107)
Grade III	6.5% (7/107)
Grade IV	24.3% (26/107)
Non-GMH	39.5% (70/177)
Cerebellar hemorrhages	9% (16/177)
Fetal growth restriction	21.3% (20/94)
Other imaging abnormalities	79.1% (140/177)
Postnatal imaging	22.6% (40/177)
Head US (No.)	72.5% (29/40)
MR imaging (No.)	87.% (35/40)
CT (No.)	52.5% (21/40)
Average maternal age at fetal MR imaging (yr)	28.02 (SD, 6.02)

as means (SDs), and categoric variables were presented as number (percentage). A 2-sample t test or 1-way ANOVA was used to detect the differences in continuous variables among different groups. The correlation among categoric variables was assessed by the χ^2 or Fisher exact test when appropriate. All analyses were performed using SAS, Version 9.4 (SAS Institute). A P value < .05 was considered statistically significant.

RESULTS
Description of Cohort
A total of 177 fetuses (85 males, 71 females, 21 unknown) met the criteria and were included in the analysis, with an incidence of 2.9% (177/6179) in our patient population. The average gestational age of 25.73 weeks (range, 16.57–37 weeks) at fetal MR imaging was characteristic of the cohort as a whole. Seventy-one percent (124/177) were singleton pregnancies, and 29.9% (53/177) were multiple gestation (50 twins and 3 triplets). The average maternal age at the time of fetal MR imaging was 28.02 (SD, 6.02) years. The most common clinical indications for fetal MR imaging included suspected brain anomaly (23.7%, 42/177), twin-twin transfusion syndrome (22.6%, 40/177), and ventriculomegaly (15.3%, 27/177). These and other descriptors of the cohort are summarized in Table 1.

Fetal MR Imaging Findings
The fetuses with ICH were broadly categorized into 2 groups: associated with the GMH and unassociated with the GMH (non-GMH). GMH was identified in 60.5% (107/177) of patients. The 107 GMHs were graded into 5 categories: grade 0 = 13, grade I = 31, grade II = 30, grade III = 7, grade IV = 26. Sixty-four percent (69/107) of GMHs were unilateral (35 right and 34 left), and 35.5% (38/107) were bilateral. However, 39.5% (70/177) of patients had non-GMH, and of those, 15.7% (11/70) had cerebellar hemorrhages. Isolated cerebellar hemorrhages were seen in

54.5% (6/11) of fetuses; the other 5 patients had additional hemorrhagic insults in the supratentorial brain. Other imaging abnormalities were seen in 79.1% (140/177) of fetuses: aqueductal stenosis ($n = 7$), Chiari II malformation ($n = 14$), twin-twin transfusion ($n = 34$), and extracranial congenital anomalies. T2 and EPI were positive for hemorrhage in 84.7% and 96.3% of all cases with positive findings, respectively (Table 2). However, T1 and DWI demonstrated 46% and 57.8% positivity, respectively. The mean ventricular size was 12.76 (SD, 7.54) mm, with 59.3% (105/177) of fetuses with ventriculomegaly (>10 mm). The mean ventricular size significantly correlated with GMH grade ($P \le$ .001) (Fig 4). There was no significant difference in mean ventricle size between GMH-versus-non-GMH groups (11.9 [SD, 6.4] mm versus 14.1 [SD, 8.8] mm, $P = .085$).

Prenatal Clinical Findings

There was no significant difference in fetal sex or maternal age between the GMH-versus-non-GMH groups ($P = .116$ and $P = .068$, respectively). The presence of fetal growth restriction and fetal Doppler abnormalities was reviewed for those fetuses that had undergone sonography at our institution or had available outside examinations for review. Fetal growth restriction was identified in 21.3% (20/94) of cases. There was no significant

Table 2: Fetal MR imaging findings

ICH Imaging Characteristics	Data ($n = 177$)
T2 (+), $n = 177$	84.7% (150/177)
T1 (+), $n = 150$	46% (69/150)
DWI (+), $n = 135$	57.8% (78/135)
EPI (+), $n = 81$	96.3% (78/81)
Ventriculomegaly (>10 mm)	59.3% (105/177)
Ventricular size (mm)	12.76 (SD, 7.54)

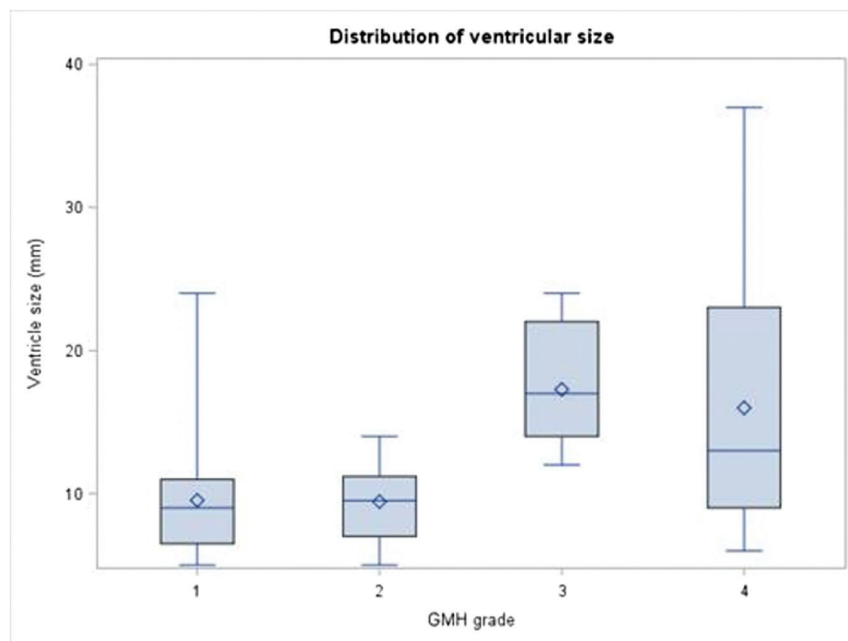**Note:—** + indicates positive imaging finding on fetal MR in those fetuses with ICH.

FIG 4. Linear regression model shows the ventricle size increased by 2.4 mm when the GMH grade increased by 1 ($P < .001$).

difference in the rate of fetal growth restriction between the GMH-versus-non-GMH groups or among the GMH grades. Fetal Doppler abnormalities were present in 43% (40/93) of fetuses with ICH, and 35% (14/40) of those were seen in the setting of twin-twin transfusion.

Postnatal Imaging Findings

A total of 40 neonates, 65% with GMH (26/40) and 35% with non-GMH (14/40), had postnatal imaging, including neonatal head US, brain MR imaging, and/or head CT examinations. Most neonates underwent >1 different imaging modality in the postnatal period. The postnatal imaging examinations overall demonstrated improvement of the prenatal ICH in most neonates, with overall decreased volume of hemorrhage (Fig 5 and Table 3). However, 3.4% (1/29) of head US, 11.4% (4/35) of brain MR imaging, and 4.8% (1/21) of head CT of neonates showed worsened findings of ICH. Postnatal head US and MR imaging showed a significant difference in brain parenchyma as correlated with GMH grade. Brain parenchymal findings were stable on head US and MR imaging, with a less severe GMH (grades 0–II) versus more severe GMH (grade III–IV); the latter demonstrated significant worsening of brain parenchymal findings, including cerebral or cerebellar white matter volume loss and/or injury and/or porencephalic cysts (Online Supplemental Data). However, the GMH grade did not significantly correlate with postnatal brain parenchymal findings on head CT. Evaluation of the brain parenchyma postnatally also showed no significant correlation between GMH-versus-non-GMH groups.

Postnatal Clinical Findings

There was a significant difference in neonatal outcome between GMH versus non-GMH ($P = .022$) when comparing those neonates who died within the first year of life with those who survived beyond the neonatal period after a live birth in the 48 fetuses who had available postnatal clinical data. Neonatal death occurred in 23% (9/40) of patients with GMH versus 50% (14/28) of those with non-GMH. However, there was not a significant difference in the delivery outcome ($P = .947$). There was also not a significant difference in the delivery or neonatal outcome among GMH grades ($P = .069$, $P = .253$). However, there was a higher incidence of death at delivery in those fetuses with grade III GMH at 57% (4/7) (grade 0 = 8%, grade I = 13%, grade II = 17%, and grade IV = 15%); 23.2% (16/69) of the neonates with available clinical data required a ventriculoperitoneal shunt. The χ^2 test revealed a statistically significant increased risk of shunt requirement in the non-GMH group compared with the GMH group ($P = .026$). Chiari II malformation was present in 40% (4/10) of the neonates
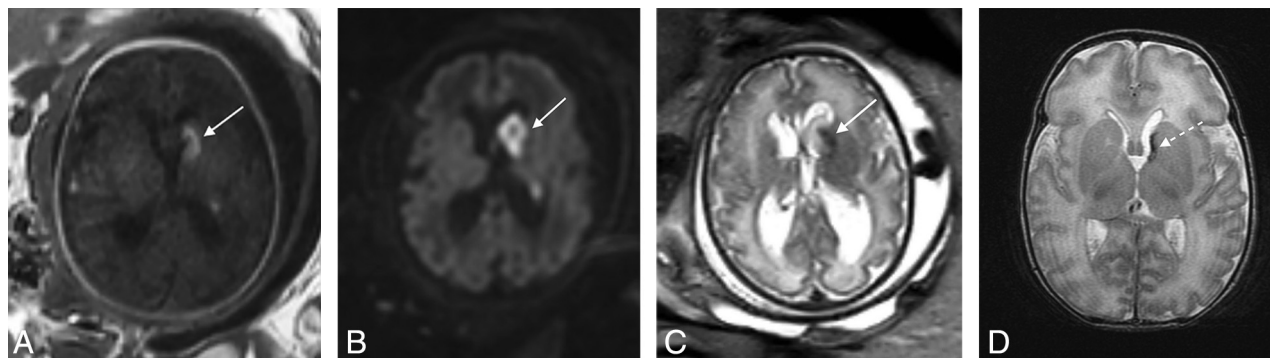
FIG 5. Left, grade IV GMH in a 35 weeks' GA fetus. Axial T1(*A*), DWI (*B*), and T2 SSFSE (*C*) images of the brain demonstrate blood products centered in the left caudothalamic groove, extending posteriorly along the left lateral ventricle with associated T1 hyperintensity, restricted diffusion, and T2 hypointensity (*arrows*). *D*, Postnatal axial T2 of the brain at day 6 of life shows decreased T2 hypointensity centered at the left caudothalamic groove (*dashed arrow, D*) compared with prenatal image (*C*), consistent with decreased volume of hemorrhage.

Table 3: Postnatal intracranial hemorrhage findings

Imaging Modality	Findings	Data
US	Same	27.6% (8/29)
	Better	69.0% (20/29)
	Worse	3.4% (1/29)
MR	Same	14.3% (5/35)
	Better	74.3% (26/35)
	Worse	11.4% (4/35)
CT	Same	0% (0/21)
	Better	95.2% (20/21)
	Worse	4.8% (1/21)

in the non-GMH group that required a ventriculoperitoneal shunt. In the GMH group, there was a significant correlation between the GMH grades and the need for shunt placement ($P = .029$). Of those neonates that required a shunt, the mean ventricle size was significantly larger than in those who did not need shunt placement (35.5 [SD, 17.2] mm versus 17.8 [SD, 15.8] mm, $P = .013$).

DISCUSSION

We examined and described imaging findings of ICH on fetal MR imaging and studied the pre- and postnatal clinical data and postnatal imaging findings in relation to the prenatal MR imaging. We made several observations: 60.5% (107/177) of fetal ICHs involved the germinal matrix and were presumed to be germinal matrix in origin. MRI sequences that were important in the identification of hemorrhage on prenatal imaging included T2 and EPI blood sequences because they were positive for hemorrhage in 84.7% (150/177) and 96.3% (78/81) of cases, respectively. There was a significant increase in the mean ventricular size as the GMH grade increased ($P \leq .001$). The neonates that had postnatal MR imaging demonstrated improved findings of ICH (74.3%, 26/35), though 51.4% (18/35) showed worsened brain parenchymal changes. Neonatal death was significantly increased in fetuses in the non-GMH compared with the GMH group ($P = .022$). However, within the GMH group, an increased incidence of neonatal death was seen in the grade III GMHs compared with the others ($P = .069$), though there was not a significant difference among the remaining grades.

Fetal ICH has been predominantly described and classified on US in the literature, with intraventricular hemorrhage the most common subtype of fetal ICH.[5,9,16,17] There are limited data of non-GMH forms of fetal ICH, including intraparenchymal hemorrhages in the cerebrum or cerebellum and subdural and subarachnoid hemorrhages. These data are further complicated by inconsistent descriptions in the literature because the true nature of parenchymal hemorrhages in the fetus and neonate is not always clear. Some report that the terms "periventricular hemorrhagic infarction" or "venous infarction" are preferred over grade IV intraventricular hemorrhage.[18] Previous studies of fetal ICH detected on US report an incidence of 0.5–0.9 of 1000 cases.[4,5] In a more recent study of fetal ICH detected on MR imaging, the incidence was higher and occurred in 1% of cases, a finding more comparable with those in our study in which fetal ICH occurred in 2.9% of our referral population.[19] The increased incidence may be the result of the increased sensitivity of MR imaging in the evaluation of ICH and/or the population of patients referred to our center.

Our results are similar to those in the study performed by Sanapo et al,[19] in which they discovered that ICH was confined to the GMH in 67% of fetuses versus a non-GMH location in the remainder (33%). Those hemorrhages that occurred in the cerebellum were classified in the non-GMH group in both studies. It is believed by some authors that cerebellar hemorrhages occur within the germinal matrix located in the subependymal layer of the roof of the fourth ventricle and in the subpial external granule cell layer.[20,21] Previously, most cerebellar hemorrhages were thought to be the result of significant birth-related trauma or associated with extensive supratentorial hemorrhage.[22,23] Given the uncertain classification of prenatal/neonatal cerebellar hemorrhages, we decided to classify those hemorrhages as non-GMH for this study.

The study of Sanapo et al[19] described ventriculomegaly in most of their cases (80%), compared with 59.3% in our study. The frequency of intrauterine fetal death was higher in the non-GMH-versus-GMH groups (58% versus 4%) in their study, and we, too, found a significant increase in neonatal death in the non-GMH group (50% versus 23%). The incidence of death in the GMH group was higher in our study, which is more comparable with the results of another study by Ghi et al,[17] in which the

authors observed a 16% incidence in death in fetuses with intraventricular hemorrhage. The etiology of the higher incidence of intrauterine fetal and neonatal death in the GMH group is unclear. However, the incidence in our study may be overestimated because a relatively large proportion of fetuses with less severe GMH (grades 0, I, and II) were lost to follow-up; therefore, the true incidence is likely much lower. Prior studies have demonstrated worse neurologic outcomes in the setting of grade III and IV GMHs.[5,17,19] Although we did not assess the long-term neurodevelopmental status of our patients, we found that more severe GMHs (grade III−IV) demonstrated worsened parenchymal findings in the postnatal setting, including cerebral or cerebellar white matter volume loss or porencephalic cysts, likely contributing to poorer neurologic outcomes.

Our study has several limitations, including the retrospective design of the study limiting its internal validity. Even though our fetal study population was relatively large, the postnatal follow-up imaging and clinical data were a much smaller sample size. Another limitation of our study was that the neurosonographic findings were not evaluated in detail. The study was also subject to some degree of selection bias because the imaging data were collected from a large tertiary care pediatric hospital, limiting the external validity of our findings. Also, the EPI blood sequence was not performed in all fetal MR imaging examinations in our study because it only became part of our routine protocol in 2016; therefore, some grade I GMHs and subtle non-GMHs could have been missed. The authors also acknowledge that the modified Burstein and Papile grading system used to classify GMHs in the fetus has its limitations because parenchymal hemorrhages and cerebellar hemorrhages may be of germinal matrix origin. However, in the absence of another widely published grading system in the fetus, we chose to use this classification system for this study. Finally, all of our examinations were performed on a 1.5T magnet, and it is plausible that use of a 3T magnet would have increased the sensitivity of the detection of ICH from increased signal-to-noise.[24]

CONCLUSIONS

Given that this is the largest single-center cohort of fetal ICH examined on MR imaging, we add several important findings to the existing literature. First, the EPI blood sequence is the most sensitive in the identification of fetal ICH, which, in conjunction with T2-SSFSE images, can allow optimizing classification and subsequent grading of GMHs in the fetus. Second, we reported a significant increase in neonatal death in the non-GMH-versus-GMH group and worsened brain parenchymal findings in more severe GMH grades (III–IV) on postnatal MR imaging. Last, we discovered a significant increased risk of shunt requirement in the non-GMH-versus-GMH group; and in those neonates that required a shunt, the mean ventricle size was significantly larger. All our findings demonstrate the importance of accurate classification of fetal ICH because it may have an impact on the therapeutic approach, prenatal/perinatal counseling, and neurologic outcomes.

REFERENCES

1. Griffiths PD, Bradburn M, Campbell MJ, et al; MERIDIAN collaborative group. **Use of MRI in the diagnosis of fetal brain abnormalities in utero (MERIDIAN): a multicentre, prospective cohort study.** *Lancet* 2017;389:538–46 CrossRef Medline
2. Glenn OA, Barkovich AJ. **Magnetic resonance imaging of the fetal brain and spine: an increasingly important tool in prenatal diagnosis, Part 1.** *AJNR Am J Neuroradiol* 2006;27:1604–11 Medline
3. Glenn OA, Barkovich J. **Magnetic resonance imaging of the fetal brain and spine: an increasingly important tool in prenatal diagnosis, part 2.** *AJNR Am J Neuroradiol* 2006;27:1807–14 Medline
4. Vergani P, Strobelt N, Locatelli A, et al. **Clinical significance of fetal intracranial hemorrhage.** *Am J Obstet Gynecol* 1996;175:536–43 CrossRef Medline
5. Elchalal U, Yagel S, Gomori JM, et al. **Fetal intracranial hemorrhage (fetal stroke): does grade matter?** *Ultrasound Obstet Gynecol* 2005;26:233–43 CrossRef Medline
6. Cheung KW, Tan LN, Seto MT, et al. **Prenatal diagnosis, management, and outcome of fetal subdural haematoma: a case report and systematic review.** *Fetal Diagn Ther* 2019;46:285–95 CrossRef Medline
7. Kline-Fath BM. Supratentorial anomalies. In: Kline-Fath BM, Bulas DI, Lee W, eds. *Fundamental and Advanced Fetal Imaging Ultrasound and MRI.* 2nd ed. Wolters Kluwer; 2021:489–95
8. Burstein J, Papile La, Burstein R. **Hemorrhage and hydrocephalus in premature newborns: study with CT.** *AJR Am J Roentgenol* 1979;132:631–35 CrossRef Medline
9. Hintz SR, Slovis T, Bulas D, et all; NICHD Neonatal Research Network. **Interobserver reliability and accuracy of cranial ultrasound scanning interpretation in premature infants.** *J Pediatr* 2007;150:592–96 CrossRef Medline
10. Huang YF, Chen WC, Tseng JJ, et al. **Fetal intracranial hemorrhage (fetal stroke): report of four antenatally diagnosed cases and review of the literature.** *Taiwan J Obstet Gynecol* 2006;45:135–41 CrossRef Medline
11. Adiego B, Martínez-Ten P, Bermejo C, et al. **Fetal intracranial hemorrhage: prenatal diagnosis and postnatal outcomes.** *J Matern Neonatal Med* 2019;32:21–30 CrossRef Medline
12. Nagaraj UD, Kline-Fath BM. **Imaging diagnosis of ventriculomegaly: fetal, neonatal, and pediatric.** *Childs Nerv Syst* 2020;36:1669–79 CrossRef Medline
13. Gordijn SJ, Beune IM, Thilaganathan B, et al. **Consensus definition of fetal growth restriction: a Delphi procedure.** *Ultrasound Obstet Gynecol* 2016;48:333–39 CrossRef Medline
14. Quintero R, Morales W, Allen M, et al. **Staging of twin-twin transfusion syndrome.** *J Perinatol* 1999;19:550–55 CrossRef Medline
15. Mari G, Deter RL, Carpenter RL, et al. **Noninvasive diagnosis by Doppler ultrasonography of fetal anemia due to maternal red-cell alloimmunization: Collaborative Group for Doppler Assessment of the Blood Velocity in Anemic Fetuses.** *Obstet Gynecol Surv* 2000;55:341–42 CrossRef Medline
16. Abdelkader MA, Ramadan W, Gabr AA, et al. **Fetal intracranial hemorrhage: sonographic criteria and merits of prenatal diagnosis.** *J Matern Neonatal Med* 2017;30:2250–56 CrossRef Medline
17. Ghi T, Simonazzi G, Perolo A, et al. **Outcome of antenatally diagnosed intracranial hemorrhage: case series and review of the literature.** *Ultrasound Obstet Gynecol* 2003;22:121–30 CrossRef Medline
18. Brouwer AJ, Groenendaal F, Benders MJNL, et al. **Early and late complications of germinal matrix-intraventricular haemorrhage in the preterm infant: what is new?** *Neonatology* 2014;106:296–303 CrossRef Medline
19. Sanapo L, Whitehead MT, Bulas DI, et al. **Fetal intracranial hemorrhage: role of fetal MRI.** *Prenat Diagn* 2017;37:827–36 CrossRef Medline

20. Haines KM, Wang W, Pierson CR. **Cerebellar hemorrhagic injury in premature infants occurs during a vulnerable developmental period and is associated with wider neuropathology.** *Acta Neuropathol Commun* 2013;1:69 CrossRef Medline

21. Merrill JD, Piecuch RE, Fell SC, et al. **A new pattern of cerebellar hemorrhages in preterm infants.** *Pediatrics* 1998;102:e62 CrossRef Medline

22. Martin R, Roessmann U, Fanaroff A. **Massive intracerebellar hemorrhage in low-birth-weight infants.** *J Pediatr* 1976;89:290–93 CrossRef Medline

23. Grunnet ML, Shields DW. **Cerebellar hemorrhage in the premature infant.** *J Pediatr* 1976;88:605–08 CrossRef

24. Weisstanner C, Gruber GM, Brugger PC, et al. **Fetal MRI at 3T-ready for routine use?** *Br J Radiol* 2017;90:20160362 CrossRef Medline